International Journal of Minerals, Metallurgy and Materials
Volume 18, Number 2, April 2011, Page 229
DOI: 10.1007/s12613-011-0427-8

Mechanism of brittle-ductile transition of a glass-ceramic rigid substrate

Yu-li Sun, Dun-wen Zuo, Hong-yu Wang, Yong-wei Zhu, and Jun Li

Jiangsu Key Laboratory of Precision and Micro-manufacturing Technology, College of Mechanical and Electrical Engineering, Nanjing University of Aeronautics and Astronautics, Nanjing 210016, China

(Received: 19 April 2010; revised: 3 June 2010; accepted: 11 July 2010)

Abstract: The hardness, elastic modulus, and scratch resistance of a glass-ceramic rigid substrate were measured by nanoindentation and nanoscratch, and the fracture toughness was measured by indentation using a Vickers indenter. The results show that the hardness and elastic modulus at a peak indentation depth of 200 nm are 9.04 and 94.70 GPa, respectively. These values reflect the properties of the glass-ceramic rigid substrate. The fracture toughness value of the glass-ceramic rigid substrate is 2.63 MPa·$m^{1/2}$. The material removal mechanisms are seen to be directly related to normal force on the tip. The critical load and scratch depth estimated from the scratch depth profile after scratching and the friction profile are 268.60 mN and 335.10 nm, respectively. If the load and scratch depth are under the critical values, the glass-ceramic rigid substrate will undergo plastic flow rather than fracture. The formula of critical depth of cut described by Bifnao *et al*. is modified based on the difference of critical scratch depth

Keywords: brittle-ductile transition; critical conditions; glass ceramics; nanoindentation; nanoscratch

[*This work was financially supported by the National Natural Science Foundation of China (No.50905086), China Postdoctoral Science Foundation (No.200904501095), Jiangsu Planned Projects for Postdoctoral Research Funds (No.0901035C), and NUAA Research Funding (No.NS2010134).*]

1. Introduction

Glass-ceramic substrates are beginning to be used in the construction of magnetic thin-film rigid disks for their rigidity, shock (dent) resistance, and smoothness over commonly used Ni-P coated aluminum-magnesium substrates [1]. Using glass-ceramic rigid substrates, the recording density and access speed of hard disks can be improved [2]. However, glass-ceramic rigid substrates need to have not only very good flatness and low surface roughness but also no surface damage and scratches. The glass-ceramic rigid substrate is a kind of hard brittle material and easy to fail in the way of wear-out failure because of brittle fracture, so it is difficult to machine this kind of hard brittle material. In recent years, many researchers have tried their best to obtain superior quality by ductile regime machining of brittle materials [3-6], but the mechanism of brittle-ductile transition of hard brittle materials still lacks in-depth study. Though a lot of indentation tests for hard brittle materials have been done by Vickers hardness tester to analyze the formation and propagation of the microcrack and its feature [7-9], in real ultraprecise machining, machining is always in dynamic state. Traditional microindentation tests are always in static state, so they cannot reflect the real ultraprecise machining. Nanoscratch is a new kind of method to visualize the transition from a brittle to a ductile mode during the real machining of brittle materials [10].

This paper aims to measure the properties of the glass-ceramic rigid substrate by the nanoindentation continuous stiffness measurement (CSM) technique and study the mechanism of brittle-ductile transition of glass-ceramic rigid substrate using nanoscratch technique.

2. Experimental

Lithium aluminosilicate (LAS) glass ceramics were used. The composition (wt%) of the glass raw materials is: Li_2O 3.5, $A1_2O_3$ 19.8, SiO_2 67.5, TiO_2 4.2, Na_2O 2.5, MgO 2.5,

Corresponding author: Dun-wen Zuo E-mail: imit505@nuaa.edu.cn

and K_2O 0.5. TiO_2 was introduced as a nucleation agent, Na_2O and K_2O were used to reduce the melting temperature and viscosity of the glass and improve the glass workability. The glass raw materials were melted in a laboratory electric furnace with Globar heating elements in quartz crucibles at 1600-1650ºC for 8 h with stirring and molded in a pre-heated die. The glass was annealed at 580ºC for 1 h and slowly cooled in the furnace to eliminate internal stress. One-, two-, and three-stage heat-treatments were carried out under isothermal conditions at 660-800ºC. The exact heat-treatment schedules were as follows: the first stage was held at 660ºC for 24 h, the second stage was held at 720ºC for 18 h, and the third stage was held at 800ºC for 12 h. The dimension of the glass ceramics is 10 mm×6 mm×1 mm. Prior to testing, the glass ceramics were cleaned by ultrasonic in acetone for 10 min, and then weathered by nitrogen gas to remove any organic contaminants. The morphologies and surface roughness of the glass ceramics were observed and examined on a non-contact surface topography instrument (ADE). The morphologies of the glass ceramic are shown in Fig. 1. It can be seen that the surface roughness of the glass ceramic is 1.00 nm within 859 μm×639 μm and its undulation is smaller.

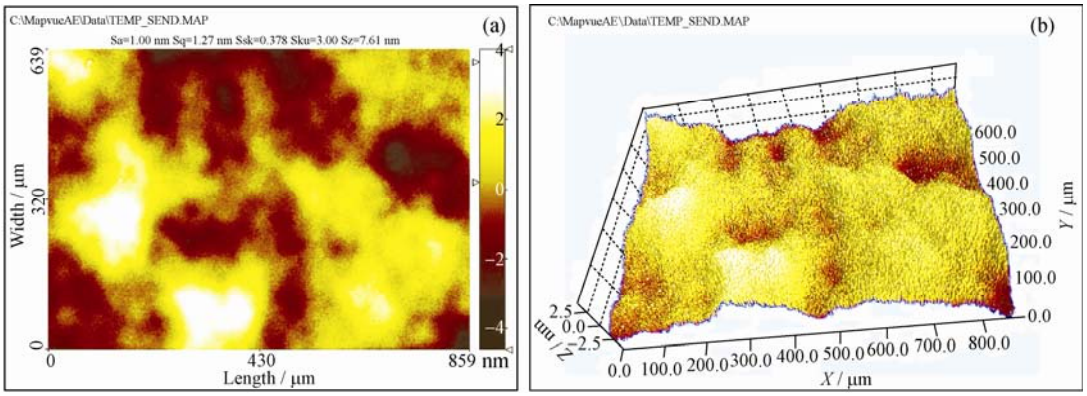

Fig. 1. Surface profile of glass ceramics before nanoindentation and nanoscratch (within 859 μm×639 μm): (a) two-dimensional pattern; (b) three-dimensional pattern.

Hardness and elastic modulus were calculated from the load-displacement data obtained by nanoindentation using a Nano Indenter XP (MTS Systems Corp.) equipped with the CSM option and the lateral force measurement (LFM) option. This instrument monitors and records the dynamic load and displacement of the three-sided pyramidal diamond (Berkovich) indenter, having a tip radius of about 50 nm and an included angle of 65.2° during indentation with a force resolution of about 50 nN and displacement resolution of about 0.01 nm. The indentation technique for fracture toughness measurement was based on the measurement of the lengths of median and radial cracks produced by indentation. A Vickers indenter (a four-sided diamond pyramid) was used in a microhardness tester. A load of 1.96 N was used in making the Vickers indentations. The indentation impressions were examined using an optical microscope with photogrammetric apparatus to measure the length of median-radial cracks.

In nanoscratch studies, the three-sided pyramidal diamond (Berkovich) indenter, having a tip radius of about 100 nm and an included angle of 65.2°, was drawn over the sample surface, and the load was ramped up, until substantial damage occurred. The friction coefficient was monitored during scratching. To obtain scratch depths during scratching, the surface profile of the glass ceramic was obtained by scanning the sample at a low load of about 100 μN, which was insufficient to damage the sample surface.

3. Results and discussion

3.1. Nanoindentation properties

The elastic modulus and hardness as a function of contact depth for the glass ceramic is shown in Fig. 2. As shown in Fig. 2, the trend that the hardness changes with contact depth is similar to that of the elastic modulus. When the contact depth is between 0 and 60 nm, the hardness increases with the increase of contact depth. Similarly, the elastic modulus also increases with increasing contact depth when the indentation is below 30 nm, due to the fact that the practical tip of the diamond indenter is of a finite radius of sharp point. This effectively sets a limit on the minimum indentation depth that is necessary to obtain reliable elastic modulus and hardness data [11]. When the indenta-

tion is more than 60 nm, the hardness and elastic modulus stay constant, on the whole. Those values reflect the properties of the glass ceramic. The hardness and elastic modulus at a peak indentation depth of 200 nm are 9.04 and 94.70 GPa, respectively.

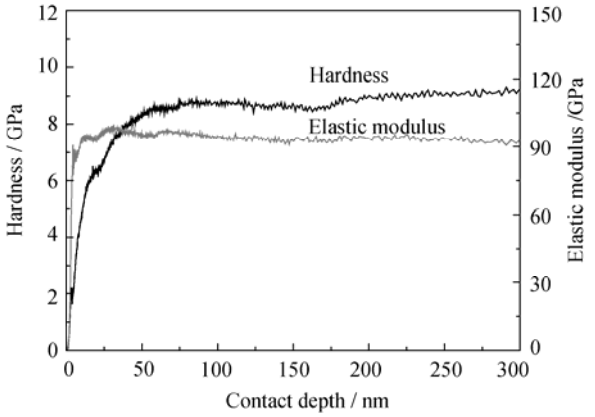

Fig. 2. Hardness and elastic modulus as a function of contact depth.

The optical image of Vickers indentations made at a normal load of 1.96 N for 10 s on the glass ceramic is shown in Fig. 3. As shown in Fig. 3, in addition to the indentation marks, radial cracks are found, emanating from the indentation corners and the radial cracks are straight. The method used to calculate the fracture toughness (K_{IC}) was developed by Lawn *et al*. [12] and it relates crack length (c) to K_{IC} as follows.

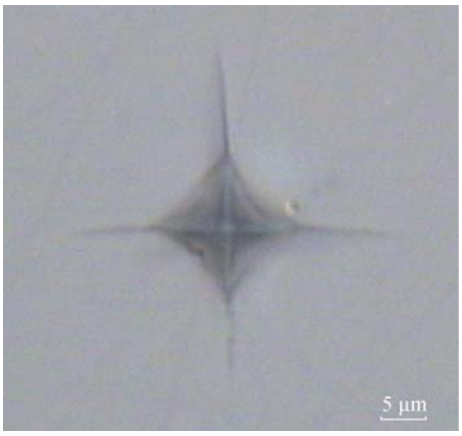

Fig. 3. Optical image of Vickers indentation made at a normal load of 200 g for 10 s.

$$K_{IC} = \alpha \left(\frac{E}{H}\right)^{1/2} \left(\frac{P}{c^{3/2}}\right) \quad (1)$$

where α is an empirical constant depending on the geometry of the indenter, E the hardness, H the elastic modulus, and P the peak indentation load. For Vickers indenters, α is empirically found based on experimental data and is equal to 0.016 [12]. Both E and H values are obtained from the nanoindentation data (Fig. 2). The crack length is measured from the center of the indent to the end of crack using an optical microscope with photogrammetric apparatus. For one indent, all crack lengths were measured. The crack length c is obtained from the average values of five indents. Based on Eq. (1), the fracture toughness value of the glass ceramic is 2.63 $MPa{\cdot}m^{1/2}$.

3.2. Nanoscratch properties

Optical images of the scratch are shown in Fig. 4. The scratch depth and friction coefficient profiles as a function of normal load and scratch distance are shown in Figs. 5 and 6, respectively. As shown in Figs. 4-6, the nanoscratch includes three stages. At the first stage, when the normal load is between 0 and 26.10 mN, the scratch depth profile obtained after the scratch does not change with respect to the initial profile, as shown in Fig. 4(a). This is attributed to an elastic recovery after the removal of normal load. The glass ceramic exhibits a continuous increase in the friction coefficient with increasing normal load from the beginning of the scratch, as shown in Fig. 5. At the second stage, when the normal load is between 26.10 and 268.60 mN, the tip plows a trough *via* plastic deformation of the glass ceramic, leaving a ductile groove, as shown in the optimal image in stage II of Fig. 4. From Fig. 5, reduction in scratch depth is observed after scratching as compared to that during scratching. This reduction in scratch depth is attributed to an elastic recovery after the removal of normal load. The glass ceramic also exhibits a continuous increase in the friction coefficient with increasing normal load, as shown in Fig. 6. The continuous increase in the friction coefficient during scratching is attributed to the increasing plowing of the sample by the tip with increasing normal load. When the normal load increases to 268.60 mN (indicated by A on the scratch depth and the friction profiles), the scratch depth profile obtained after the scratch on the glass ceramic and the friction coefficient begin to fluctuate. The optimal image of stage III shows that there are many cracks on the side of the scratch right from the load of 268.60 mN, which is probably responsible for the fluctuation in the scratch depth and the friction profiles. The scratch depth after scratching indicates the final depth which reflects the extent of permanent damage and plowing of the tip into the sample surface, and is probably more relevant for visualizing the damage that can occur in real machining [13]. For the glass ceramic, there is a large discreteness in the scratch depth data after the load of 268.6 mN, which is associated with the generation of cracks,

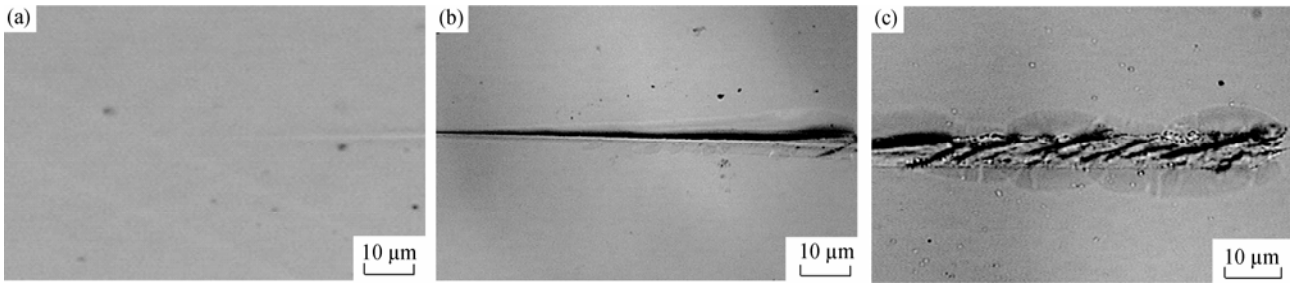

Fig. 4. SEM images of the scratch: (a) stage I; (b) stage II; (c) stage III.

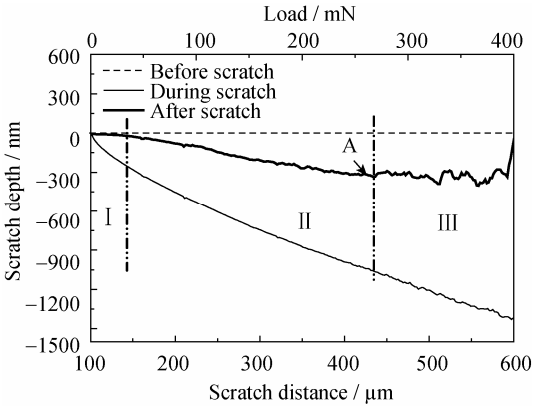

Fig. 5. Scratch depth as a function of normal load and scratch distance.

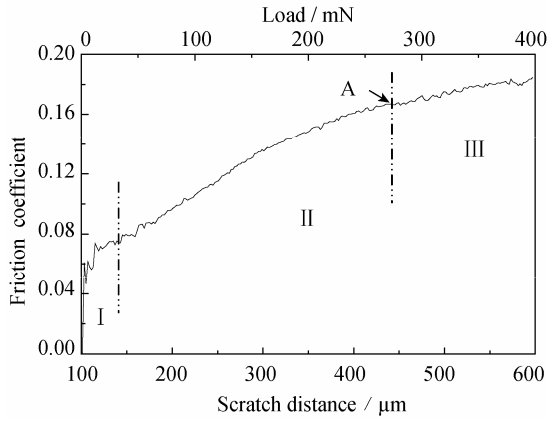

Fig. 6. Coefficient of friction as a function of normal load and scratch distance.

material removal and debris. Therefore, the critical load and scratch depth estimated from the scratch depth profile after scratching and the friction profile are 268.60 mN and 335.10 nm, respectively.

3.3. Critical depth of cut

The transition from a brittle to a ductile mode during the machining of brittle materials is described in terms of energy balance between the strain energy and the surface energy [14]. Localised fractures produced during the application of cutting force are of interest in the machining of brittle materials. Machining is an indentation process and during this indentation cracks are generated. These cracks play an important role in ductile regime machining.

The critical indentation depth (d_c) for fracture initiation is described as follows [15]:

$$d_c = b\left(\frac{E}{H}\right)\left(\frac{K_{IC}}{H}\right)^2 \tag{2}$$

where b is a constant.

Bifnao *et al*. [14] established a correlation between the calculated critical depth of cut and the measured critical-grinding-infeed-rate (*i.e.*, the grinding infeed that will produce 10% surface fracture). From this correlation, the constant of proportionality for Eq. (2) can be estimated.

$$d_c = 0.15\left(\frac{E}{H}\right)\left(\frac{K_{IC}}{H}\right)^2 \tag{3}$$

Substituting E=94.70 GPa, H=9.04 GPa, and K_{IC}=2.63 MPa·m$^{1/2}$ obtained from our experiment into Eq. (3), one obtains d_c=133.00 nm. This value is very different from the critical depth (d_c = 335.10 nm) obtained from the nanoscratch. Reasons for the difference are analyzed as follows. First, the basic hypothesis of ductile-regime grinding (*i.e.*, brittle-ductile transition for a reduced infeed rate) is only validated for fused silica by a series of grinding tests. Second, using SEM, a grid counting technique is devised to quantify the real percentage of surface fracture [14], but this grid-counting technique is somewhat subjective. In addition, the relevant properties are measured for each material using microindentation techniques; however, we measured the hardness and elastic modulus of the glass ceramic using nanoindentation techniques. The measurement of hardness by indentation is a standard procedure, while the determination of K_{IC} and E by indentation is a developing area of research. The properties of the material surface vary with indentation depth at which they are measured. This surface property variability is especially troubling for the measurement of K_{IC}. Size-scale effects lead to a dependence of K_{IC} on crack size (R-curve behavior), which can be a large effect in certain materials. Such material-related property variations complicate the extrapolation

of properties from the scale of indentation (~10 μm) to the scale of microgrinding (<1 μm). Finally, Eq. (3) is obtained in the static state, but in real work, machining is always in a dynamic condition. Therefore, Eq. (3) is only an empirical formula based on a series of grinding tests for fused silica. Materials exhibiting significant variations in K_{IC} with indentation depth are not well represented by the model. Therefore, substituting E=94.70 GPa, H=9.04 GPa, and K_{IC}=2.63 MPa·m$^{1/2}$ obtained from our experiment into Eq. (2), the constant of proportionality for Eq. (3) can be modified.

$$d_c = 0.38\left(\frac{E}{H}\right)\left(\frac{K_{IC}}{H}\right)^2 \tag{4}$$

4. Conclusions

(1) The hardness and elastic modulus at a peak indentation depth of 200 nm are 9.04 and 94.70 GPa, respectively. These values reflect the properties of the glass ceramic.

(2) The indentation technique for fracture toughness measurement is based on the measurement of the length of median-radial cracks produced by indentation. The fracture toughness value of the glass ceramic is 2.63 MPa·m$^{1/2}$.

(3) The material removal mechanisms consist of elastic deformation, plastic grooving, and crushing. The material removal mechanisms are seen to be directly related to normal force on the tip. The critical load and scratch depth estimated from the scratch depth profile after scratching and the friction profile are 268.60 mN and 335.10 nm, respectively. If the load and scratch depth are under the critical values, the glass ceramic will undergo plastic flow rather than fracture.

(4) Based on the properties of glass ceramic obtained from the experiment, the formula of critical depth of cut described by Bifnao *et al*. is modified.

References

[1] B. Bhushan, L.S. Yang, C. Gao, *et al*., Friction and wear studies of magnetic thin-film rigid disks with glass-ceramic, glass and aluminum-magnesium substrates, *Wear*, 190(1995), No.1, p.44.

[2] H.C. Tsai, Advantages and challenge of nonmetallic substrates for rigid disk applications, *IEEE Trans. Magn.*, 29(1993), No.1, p.241.

[3] J. Tamaki, A. Kubo, and J.W Yan, Experimental analysis of elastic and plastic behavior in ductile-regime machining of glass quartz utilizing a diamond tool, *Key Eng. Mater.*, 389-390(2009), p.30.

[4] J.A. Patten and J. Jacob, Comparison between numerical simulations and experiments for single-point diamond turning of single-crystal silicon carbide, *J. Manuf. Processes*, 10(2008), No.1, p.28.

[5] D.E. Brehl and T.A. Dow, Review of vibration-assisted machining, *Precis. Eng.*, 32(2008), No.3, p.153.

[6] Rusnaldy, T.J. Ko, and H.S. Kim, An experimental study on microcutting of silicon using a micromilling machine, *Int. J. Adv. Manuf. Technol.*, 39(2008), No.1, p.85.

[7] Y.Y. Tang, A. Yonezu, N. Ogasawara, N. Chiba, and X. Chen, On radial crack and half-penny crack induced by Vickers indentation, *Proc. R. Soc. A*, 464(2008), No.2099, p.2967.

[8] X. Chen, J.W. Hntchineon, and A.G. Evane, The mechanics of indentation induced lateral cracking, *J. Am. Ceram. Soc.*, 88(2005), No.5, p.1233.

[9] K.Y. Zeng, Y.S. Pang, L. Shen, K.K. Rajan, and L.C. Lim, Elastic modulus, hardness and fracture behavior of $Pb(Zn_{1/3}Nb_{2/3}O_3)$-$PbTiO_3$ single crystal, *Mater. Sci. Eng. A*, 472(2008), No.1-2, p.35.

[10] Y.L. Sun, D.W. Zuo, D.S. Li, R.F. Chen, and M. Wang, Mechanism of brittle-ductile transition of single silicon wafer using nanoindentation techniques, *Key Eng. Mater.*, 375-376 (2008), p.52.

[11] X.D. Li, B. Bhushan, K. Takashima, C.W. Baek, and Y.K. Kim, Mechanical characterization of micro/nanoscale structures for MEMS/NEMS applications using nanoindentation techniques, *Ultramicroscopy*, 97(2003), No.1-4, p.481.

[12] B.R. Lawn, A.G. Evans, and D.B. Marshall, Elastic/plastic indentation damage in ceramics: The median/radial crack system, *J. Am. Ceram. Soc.*, 63(1980), No.9-10, p.574.

[13] D.W. Zuo, Y.L. Sun, Y.F. Zhao, and Y.W. Zhu, Basic research on polishing with ice bonded nanoabrasive pad, *J. Vac. Sci. Technol. B*, 27(2009), No.3, p.1514.

[14] T.G. Bifano, T.G. Dow, and R.O. Scattergood, Ductile-regime grinding: A new technology for machining brittle materials, *J. Eng. Ind.*, 113(1991), No.2, p.184.

[15] V.C. Venkatesh, I. Inasaki, H.K. Toenshoff, T. Nakagawa, and I.D. Marinescu, Observations on polishing and ultraprecision machining of semiconductor substrate materials, *CIRP Ann. Manuf. Technol.*, 44(1995), No.2, p.611.